ChemPubSoc Europe

DOI: 10.1002/cssc.201800318

CHEMSUSCHEM Full Papers

Controlled Selectivity of CO_2 Reduction on Copper by Pulsing the Electrochemical Potential

Kevin W. Kimura,[a] Kevin E. Fritz,[b] Jiyoon Kim,[b] Jin Suntivich,[b] Héctor D. Abruña,[c] and Tobias Hanrath*[a]

We demonstrate a simple strategy to enhance the CO_2 reduction reaction (CO_2RR) selectivity by applying a pulsed electrochemical potential to a polycrystalline copper electrode. By controlling the pulse duration, we show that the hydrogen evolution reaction (HER) is highly suppressed to a fraction of the original value (<5% faradaic efficiency) and selectivity for the CO_2RR dramatically improves (>75% CH_4 and >50% CO faradaic efficiency). We attribute the improved CO_2RR selectivity to a dynamically rearranging surface coverage of hydrogen and intermediate species during the pulsing. Our finding provides new insights into the interplay of transport and reaction processes as well as timescales of competing pathways to enable new opportunities to tune CO_2RR selectivity by adjusting the pulse profile. Additionally, the pulsed potential method we describe can be easily applied to other catalysts materials to improve their CO_2RR selectivity.

Introduction

The electrochemical CO_2 reduction reaction (CO_2RR) has garnered strong interest for converting CO_2 emissions into higher-value chemicals, including fuels and hydrocarbon feedstocks.[1,2] Aqueous electrochemical CO_2RR has the benefit of being performed at room temperature and can be powered with renewable energy sources.[3] Currently, poor selectivity control of the reaction products remains a major hurdle.[4,5] An ideal catalyst would yield one CO_2RR product and have no selectivity towards the competing hydrogen evolution reaction (HER).[6] Among the metal electrodes studied,[7] copper has emerged as one of the most promising catalysts by virtue of its ability to produce higher-order hydrocarbons.[8,9] However, copper suffers from poor selectivity and a significant portion of the reduction current goes to HER [30–80% faradaic efficiency (FE), Figure 1].[8] Although various pathways to explain the diversity of observed products have been proposed,[10,11] overcoming the selectivity toward the HER persists as a critical challenge owing to gaps in our understanding of the reaction mechanism.[12,13]

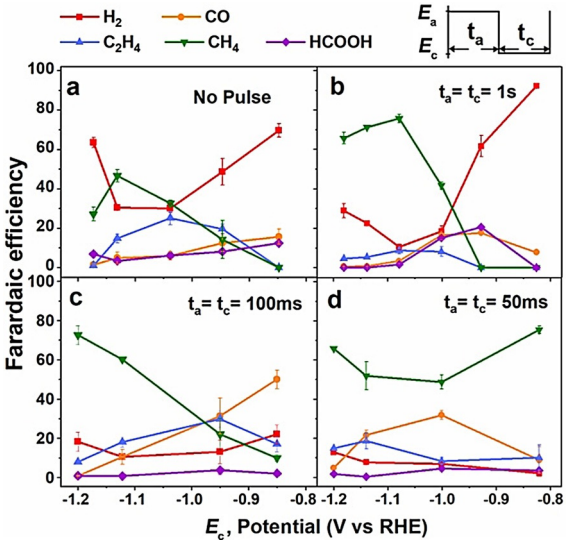

Figure 1. Faradaic efficiency for major products as a function of cathode ceiling potential (E_c). a) Constant potential. b) Pulsed potential cathodic interval (t_c) = anodic interval (t_a) = 1 s. c) Pulsed potential $t_c = t_a = 100$ ms. d) pulsed potential $t_c = t_a = 50$ ms. Pulsed potential experiments used a +0.6 V vs. RHE anode ceiling potential (E_a).

Kumar et al.[14] recently reported that tuning the temporal profile of anodic and cathodic pulses applied to a copper electrode mainly increased the FE of the HER and selectively produced CO. However, questions concerning how electrochemical pulses can control product selectivity remain. Realizing that controlling pulsing profiles may provide an effective means towards understanding and controlling the selectivity challenge, we examined how the temporal duration of an electrochemical pulse can affect product selectivity in the CO_2RR. Contrary to the results of Kumar et al., we found that a pulsed potential significantly suppressed the HER FE and increased the selectivity toward CH_4 and/or CO. This difference in the product selectivity is owing, at least in part, to the use of small electrodes,

[a] K. W. Kimura, Dr. T. Hanrath
Robert Frederick Smith School of Chemical and Biomolecular Engineering
Cornell University
Ithaca, New York (USA)
E-mail: th358@cornell.edu

[b] K. E. Fritz, J. Kim, Dr. J. Suntivich
Department of Materials Science and Engineering
Cornell University
Ithaca, New York (USA)

[c] Dr. H. D. Abruña
Department of Chemistry & Chemical Biology
Baker Laboratory, Cornell University
Ithaca, New York (USA)

The ORCID identification number(s) for the author(s) of this article can be found under:
https://doi.org/10.1002/cssc.201800318.

which have a faster electrochemical response. When using a larger electrode, we reproduced the results of Kumar et al.

Here we present our findings and hypothesis to explain the increased product selectivity. The improved fundamental understanding of this effect can help to guide future efforts towards new prospects for more selective CO_2RR electrocatalysts.

Results

We used a standard three-electrode electrochemical setup, following procedures established by previous electrochemical CO_2RR studies.[15] Details of the experimental setup are provided in the Supporting Information. Figure 1a shows a FE "baseline" for our copper working electrode under constant potential, which is consistent with previous studies.[8] We analyzed the composition of reaction products via gas chromatography (GC) and high-performance liquid chromatography (HPLC). We focused on detecting H_2, CO, CH_4 and C_2H_4, and HCOOH, as these major products are known to compose ≈90–98% of the FE.[15]

We modulated the square-wave potential by varying pulse widths to examine how pulse duration affects the CO_2RR selectivity. Using a 0.1 cm^2 copper electrode, we kept the anodic potential ceiling (E_a) at 0 V vs. Ag/AgCl [+0.6 V vs. the reversible hydrogen electrode (RHE)] and varied the reduction potential ceiling (E_c). The cathodic and anodic pulse intervals were kept symmetric (i.e., $t_c = t_a$). The resulting product distributions were compared to the baseline FEs. Figure 1b–d shows the FE for pulse intervals of 1 s, 100, and 50 ms, respectively. Results for shorter pulse intervals (20 and 10 ms) are available in the Supporting Information. Remarkably, the HER is suppressed at all measured potentials more negative than −1 V vs. RHE for the 1 s pulse and all measured potentials for the millisecond pulse intervals. Furthermore, CH_4 is selectively favored for all pulse intervals, especially for potentials more negative than −1.0 V vs. RHE. For the 50 ms pulse, CH_4 FE dominated throughout the potential window. The selectivity for CO is favored in comparison to the baseline for less negative potentials (e.g, at 100 ms and −0.85 V vs. RHE). In the case of the 20 ms pulse, the HER FE decreased by a factor of 8 at −1 V vs. RHE (Figure S1b).

We determined current density for each product under different pulse conditions by averaging the faradaic current segment of each pulse and normalizing it by the electrode area (Figure S5). Figure 2a shows the total faradaic current density for each pulse interval over the voltage ranges tested. In general, the total current densities were insensitive to the studied pulse intervals. Figure 2b and c show the current density for CH_4 and H_2 respectively. For potentials more negative than −1 V vs. RHE, the use of pulses increased the current density for CH_4 and suppressed the HER. The FE change in Figure 1 is therefore not solely a result of either an increase in CH_4 or a decrease in the HER alone. Rather, both effects are concurrent. Current densities for the other products are provided in Figure S2.

The analysis of transient currents in chronoamperometric studies requires careful consideration of the electrode geometry to differentiate faradaic processes at the electrode surfaces from induction transients of the overall system. One of the primary differences in the experimental setup between our work and the previous report by Kumar et al.[14] is the area of the copper working electrode. Notably, Kumar et al. used a larger electrode area (≈5 cm^2) in comparison to ours (0.1 cm^2). To determine the origin of the dramatic difference in product selectivity between our results, we compared different electrode/electrolyte interface area geometries. We varied the working and counter electrode surface area and compared the transient current in response to the potential pulse. Figure 3a illustrates the importance of using a high counter/working electrode surface area ratio to properly study current transients that are not obscured by induction artifacts. The red trace in Figure 3a shows the transient current for the large (5 cm^2) working electrode with small counter electrode/working electrode area ratio (1:1). This causes a noticeable induction period, which can vary depending on the system. The black line is the same 5 cm^2 working electrode with a much large ratio of counter/working (50:1). Figure 3b is the current for the small electrode (0.1 cm^2), which has no induction time and short double-layer charging.

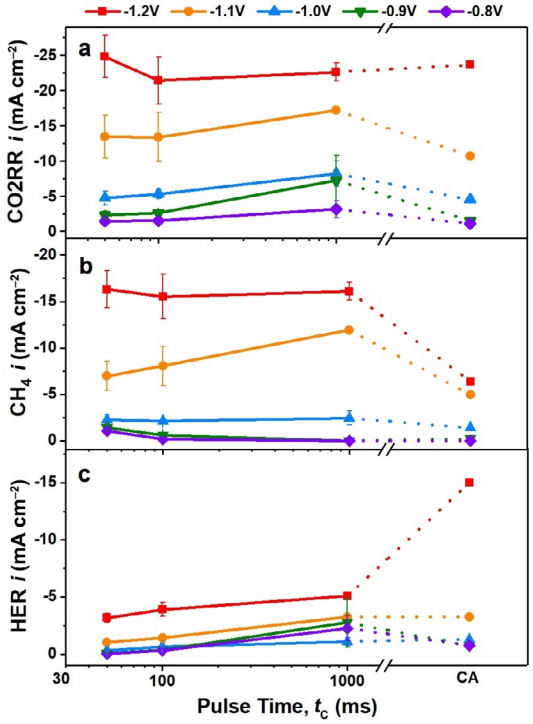

Figure 2. Current densities of specific products for constant (CA) and pulsed potentials at various reduction voltages [cathode potential ceiling (E_c)]. Faradaic current density for a) CO_2RR, b) CH_4, and c) HER.

Additionally, the performance of the 5 cm^2 electrode was tested using 100 ms pulses (Figure S7). The FE of H_2 and CO on the large area electrodes (5 cm^2) were consistent with previous literature,[14] which is drastically different from the results of smaller (0.1 cm^2) electrodes shown in in Figure 1. The relatively small electrodes used in our experiments (0.1 cm^2) have no induction time and relatively fast double-layer charging, which

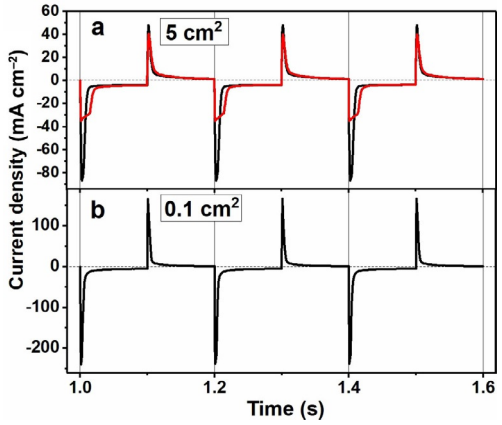

Figure 3. Pulse profile (black line) of current density for a) 5 cm^2 and b) 0.1 cm^2 working electrode with a counter/working electrode area ratio of 50:1. Red line current profile in Figure 3a results from counter/working = 1:1.

leads to the shortest transient time ($\Delta\tau$). Given the pronounced dependence of product selectivity on electrode area, we infer that $\Delta\tau$ affects the product output. Additional experiments conducted by varying the counter-to-working-electrode distance and changing the electrolyte volume had little effect on the product distributions.

To gain deeper insights into the underlying mechanism, we performed the CO reduction reaction (CORR), in addition to the CO_2RR experiments. CO gas was bubbled into the cell at the same flow rate as the CO_2 previously tested with CO compatible fittings. All other experimental conditions were kept constant during the CO reduction tests. The major products observed during CORR were CH_4, C_2H_4, and H_2.[16] Figure 4 shows the CORR results, comparing constant potential and 1 s cathodic/anodic pulse intervals.

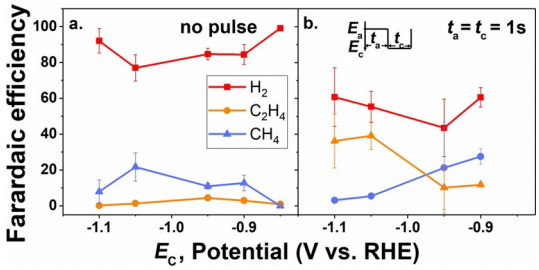

Figure 4. FE of major products for CORR. a) Constant potential. b) Pulsed potential $t_c = t_a = 1$ s.

Discussion

The fact that the electrochemical potential pulse profile can influence the reaction product selectivity raises several important questions about the interplay between and relative contribution of surface reactions and mass-transport processes. In contrast to previous studies of pulsed potential electrochemical CO_2RR,[14,17] we report a pronounced HER suppression and increased CH_4 and CO selectivity. To explain this effect, we considered three hypotheses: 1) the effect of pulsed potentials on mass transport to/from the electrode, 2) dynamic reconstruction of the electrode surface, and 3) the influence of surface concentrations on the dominant reaction pathway. We note that all three processes are not exclusive, but more likely operative to different degrees during the experiment. Accordingly, our discussion below focuses on describing which process is dominant.

If the suppression of HER during the pulsing is interpreted as improved mass transport of CO_2 to the electrode surface, one would expect to see a uniform increase in FE for all the hydrocarbon products. Contrary to this prediction, we observe a selective increase in the CH_4 FE for more negative potentials and CO at less negative potentials, indicating pulsing-dependent product selectivity is not solely a mass transport phenomenon.

We performed rotating disk electrode (RDE) experiments to better understand the relative contribution of mass transport and surface reaction processes (Figure S8). The RDE results in Section S8 of the Supporting Information reveal two important contrasting trends: i) in the case of a constant potential, rotating the electrode decreases the selectivity towards CO_2RR, whereas ii) in the case of a pulsed potential (50 ms), the opposite trend is observed; CO_2RR increases when transport is enhanced by rotating the electrode. Although the enhanced HER at a rotated electrode at a constant potential is consistent with a previous report by Lim et al.,[18] the suppressed HER in the case of a rotated and pulsed electrode suggests that other transport processes dominate. Rotating the electrode improves transport of all species (i.e., H_3O^+, CO_2, and CO) to and from the electrode surface. In the case of a static potential, the increased HER at a rotated electrode can be interpreted as improved transport of H_3O^+ to or CO from the electrode surface. The relative enhancement of the H_3O^+ concentration near the surface dominates over concurrent enhancement in CO_2 concentration. To explain the suppressed HER at a rotated and pulsed electrode surface, another mechanism must be operative. Specifically, we interpret the suppressed HER (at rotated and pulsed electrodes) as an indication that the average (i.e., time integrated) H_3O^+ concentration is lower compared to the rotated electrode at constant potential.

To better understand how the concentrations of reactants and products change in the boundary layer near the electrode surface, we turned to analytical modeling of the underlying transport and reaction processes. The diffusion model was adapted from Gupta et al.[19] by applying a millisecond time-scale piece-wise boundary condition to simulate the pulsing. Figure S8 shows calculated concentrations of CO_2 and other equilibrium species at the boundary layer. The concentration of CO_2 at the surface of the electrode pulsed at 50 ms is similar to the constant potential case. In contrast, calculations with longer pulse times (i.e., 5 s or longer) predict a higher averaged CO_2 concentration at the surface. Whereas the millisecond pulse intervals dramatically improved CO_2RR selectivity, 5 s and longer pulse intervals exhibited product selectivity behavior similar to that of the constant potential case. In short, the analytical model suggests that the pulse-dependent product

selectivity for short pulse width (50 ms) is not a result of enhanced CO_2 concentration in the boundary layer, hence improved mass transport is not the primary mechanism behind the effect that we have observed.

Modulating the pulse profile to control the H_2:CO product ratio was interpreted by Kumar et al.[14] as a changing Helmholtz layer to promote CO desorption. Oxidation of copper during the anodic pulse was also hypothesized to roughen the surface, favoring CO production. Finally, at longer millisecond pulses, improved mass transport was suggested to favor CO_2RR selectivity. This interpretation does not explain our findings when using a smaller electrode, as we found significantly less H_2 for most tested potentials and longer pulses did not lead to improved CO_2RR FE. Instead, we hypothesize that the observed product selectivity is affected by the dynamic (time-dependent) coverage of surface species during potential pulsing, as depicted in the cartoon in Figure 5. It is well-accepted

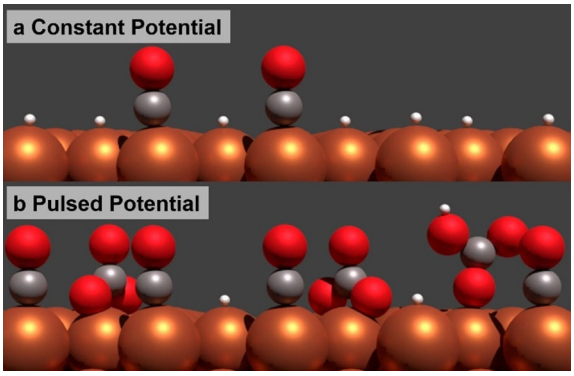

Figure 5. Conceptual depiction of adsorbed species on the copper electrode surface. Note: black, red, white, and brown represent C, O, H, and Cu respectively. a) High proton surface passivation during a constant reduction potential. b) High CO and carbonate surface passivation during a pulsed potential.

that the surface affinity of CO determines the reduction of CO_2 and product selectivity.[20] During the cycle of the anodic pulse at +0.6 V vs. RHE, the electro-adsorbed hydrogen can preferentially electro-desorb ($H_{ad} \rightarrow H^+ + e^-$), compared to other intermediates.[11] This drives the hypothesis that surface hydrogen coverage is lowered through each anodic pulse.[2,21] As surface hydrogen is known to be a HER intermediate, lowering its coverage would suppress the HER. Additionally, in situ FTIR experiments have shown that CO and CO_3^{2-} adsorb at positive potentials;[22,23] therefore, the pulsed electrode will preferentially accumulate CO_2 intermediates, over hydrogen, as depicted in Figure 5b. It is possible that during each anodic pulse the H_{ads} are being displaced by $CO_3^{2-}{}_{ads}$, which helps to suppress HER. Furthermore, the experimental results from Figures 4a and b indicate that the pulsing mechanism also suppresses HER during CORR. The HER FE is clearly lower when an anodic/cathodic pulse interval of 1 s is applied at various cathodic potentials. These results suggest that the pulsing effect is not limited to specifically CO_2 and supports the CO surface coverage hypothesis described above. For simplicity we have denoted hydrogen as a single species, however in reality it may be better represented as a hydronium ion.

We also note that surface hydrogen and hydronium near the copper surface can also react with CO_{ad} or other intermediates and thereby influence reaction pathways to selectively favor certain products.[19,21] However, based on the calculation of chemical species (specifically pH) in Figure S9, the millisecond pulse intervals exhibit similar concentration profiles to those of the constant potential experiments. Therefore, the mechanistic consequences of pulsing are likely owing to some catalyst surface phenomenon and not local concentration variations.

It is important to note that the proposed hypothesis regarding the dynamic surface coverage has many questions unanswered. Most notably, it is unclear specifically which, if any, bound species (e.g., protons, CO, carbonates) affect the product selectivity. We admit this proposed hypothesis still needs to be further examined along with other mechanisms, ideally utilizing in situ methods.

A recent report by Gunathunge et al. suggests that reversible restructuring of the surface facets during the reduction can influence the product selectivity.[24] Interestingly, the restructuring appears to occur at timescales comparable to the pulse duration. Disentangling the role of the pulse profile on dynamic changes to the physical and chemical (i.e., oxidation state)[25] electrode structure still needs to be thoroughly examined in future in situ studies.

To probe whether oxidation of the Cu surface during the anodic pulse could influence the reaction process, we examined the effects of pulsing the potential, at 50 ms pulse intervals, to various anodic potentials below +0.6 V vs. RHE; the results are shown in Figure S9. Even when the anodic potential limit was +0.2 V vs. RHE, improved CO_2RR selectivity could still be observed. At this potential, there is no CuO formation, which suggests that oxide formation may not be the primary reason behind the pulsing effect. These insights can provide a route toward understanding, and ultimately controlling, how to selectively increase the yield of a desired product. We hope to build on these results in future in situ studies to investigate the surface structuring of the metal.

The preceding proposed mechanism for HER suppression becomes negated with increasing electrode size as seen in the difference in products for the small electrode (Figure 1) and the large electrode (Figure S6). The 5 cm^2 electrode has a high selectivity for H_2 and CO for the same potentials and pulse durations. Based on the observation that an increasing electrode area increases $\Delta\tau$ (Figure 3), it is clear that larger electrodes take longer to reach the faradaic current regime (i.e., not double-layer current). The fact that the longer transient current regime correlated to larger electrodes can be attributed, at least in part, to the electrochemical system struggling to match the large working electrode's cathodic reaction, either as a result of insufficient diffusion or the large polarization needed to support the working electrode's current. The small electrode does not suffer from this transient response (short $\Delta\tau$) and quickly reaches transport-limited behavior, resulting in significantly higher CO_2RR selectivity. A crucial detail to this

pulsing mechanism is that the electrochemical system must be sufficiently fast in response to the cycling potential.

We expect that chronoamperometric studies, combined with in situ spectroscopic probes can provide more in-depth insights into the fundamental reaction rates and mechanistic pathways.[23] Furthermore, the relatively simple nature of pulsed potentials facilitates the adaptation of this technique to new electrode materials.[7,26] From an applied perspective, operating an electrolytic CO_2RR cell with pulsed potentials has important implications for on-demand selectivity control[26] and surface poisoning/fouling mitigation, the latter of which can improve long-term stability.[17] It is important to note that resistive heating induced by rapid charging/discharging would be an engineering challenge to overcome in the future.

Conclusions

We have shown that electrochemically pulsing the potential between +0.6 V vs. reversible hydrogen electrode (RHE) and a desired reduction potential can suppress the hydrogen evolution reaction (HER) and increase CO_2 reduction reaction (CO_2RR) selectivity. Millisecond pulse intervals to highly negative potentials favored CH_4, while short pulse intervals to less negative potentials favored CO production. We hypothesize the suppression of the HER in the context of preferential desorption of protons from the copper surface and accumulation of cabonate/CO_{ad} during the anodic pulsing. We combined rotating disk electrode measurements and computational modeling to show that mass-transport phenomenon is not a dominant factor in determining the pulse-dependent product selectivity. Our work points to an opportunity to discern the challenges underlying the CO_2RR selectivity on an electrode material by using the concept of controlled pulsed potentials. This technique can be easily adapted to other catalyst materials/architectures and used to probe the reaction rates and fundamental pathways in the CO_2RR.

Experimental Section

Copper electrode preparation

Annealed polycrystalline copper foil (0.127 mm thick, 99.9%, Alfa Aesar) was used as received for the working electrode. A titanium wire was attached to the copper with silver epoxy and everything except the desired copper area was covered in an inert epoxy (Omegabond 101). The copper electrode was then electropolished in 85% phosphoric acid for 1 s at 1 A cm^{-2} to achieve a mirror finish.[20] The electrode was then thoroughly rinsed in a continuous stream of deionized water for 30 s and immediately placed into the electrochemical cell.

Electrochemistry

A custom-built glass H-cell was used to perform the electrochemical measurements. A Nafion 117 membrane separated the analyte and catholyte chambers, which both held solutions of 0.1 M $KHCO_3$ electrolyte. The catholyte chamber was filled with 15 mL of electrolyte and vigorously bubbled with instrument grade CO_2 (Airgas) for 30 min to saturate the solution and reached a pH of 6.8. CO_2 gas was not bubbled into the analyte chamber.

A standard three-electrode setup was used. The counter electrode (platinum mesh area ≈12 cm^2) was placed in the analyte chamber, and the reference electrode (Ag/AgCl) and working electrode was placed in the catholyte chamber. During the experiment, CO_2 gas was bubbled in at a controlled rate of 1 mL min^{-1} and the air-tight cell had a gas outlet to the gas chromatograph. Parafilm and air-tight connections were used to ensure the whole setup did not leak gas. The system was purged with CO_2 prior to any electrochemistry experiments and held at a slight positive pressure to prevent atmospheric contamination.

A Bio-Logic SP-300 potentiostat was used with EC-Lab to perform the electrochemical measurements. The potentials for the cyclic voltammetry, chronoamperometry, and continuous double potential step chronoamperometry (pulsing) data was set with a Ag/AgCl reference electrode and later converted to a RHE scale according to the Nernst equation: $V_{RHE} = V_{Ag/AgCl} + 0.197 + 0.059 \times 6.8_{(pH)}$.[28] The potentiostat and software compensated for 85% of the value of uncompensated resistance (R_u). The other 15% was post-corrected to arrive at accurate potentials. Using impedance spectroscopy, a resistance of 160 Ω and from cyclic voltammetry, a capacitance of 15 μF was typically observed.

Product analysis

The gas products reported were measured by gas chromatography (GC, SRI Instruments Multiple Gas Analyzer #5) equipped with a thermal conductivity detector (TCD) and flame ionization detector (FID). Ultra high purity argon (Airgas) was used as the carrier gas and a hydrogen generator (H2-100, SRI Instruments) was used for the FID. The electrochemical cell was directly connected to the GC; therefore, during the electrochemistry, gases continuously flowed through regardless of sampling. Gas was sampled from the reaction vessel 20 min after applying the reducing potential. Three more samples were subsequently measured in 30 min intervals. The sampled gases took 20 min to separate through the GC columns and a 10 min rest period was applied to flush the GC. Calibration gases (Matheson and Airgas) at various dilutions were used established calibration curves for accurate product detection. Liquid products were measured by HPLC (B78 Shimadzu, Aminex HPX-87H Column) equipped with a refractive index detector (RID) to detect liquid products, specifically formic acid. Calibration curves were established using accurately measured dilutions of the liquid product. The five major products (i.e., H_2, CO, CH_4 and C_2H_4, and HCOOH) were the primary focus of detection. Other products, such as ethanol, were produced in negligible quantities.[15]

The GC samples contained 10 mL of gas each run. With a CO_2 bubbling rate of 1 mL min^{-1} and a cathodic/anodic pulse interval of 50 ms, each GC measurement would sample 6000 pulse sequences. Steady state was achieved within the first 20 min of the experiment and the ratio of products generally stayed constant throughout the four GC measurements. Two-hour experiments are typically double the length of time for experiments published in the literature. This extended time was chosen to ensure a fair average could be measured and decrease the possibility of random error.

Acknowledgements

This work was supported in part by ACS-PRF 'New Directions' grant (PRF 54130-ND5) and the National Science Foundation (NSF) under Grant No. CHE-1665305. K.W.K. was supported by the

NSF Graduate Research Fellowship. This work made use of the Cornell Center for Materials Research Shared Facilities which are supported through the NSF MRSEC program (DMR-1120296). We would like to thank Jessica Akemi Cimada DaSilva for helping to setup the GC, and David Wise for the custom cell fabrication.

Conflict of interest

The authors declare no conflict of interest.

Keywords: CO_2 · copper · electrochemical · pulsed potential · reduction

[1] E. V. Kondratenko, G. Mul, J. Baltrusaitis, G. O. Larrazábal, J. Pérez-Ramírez, *Energy Environ. Sci.* **2013**, *6*, 3112.
[2] Y. Hori in *Modern aspects of electrochemistry*, Springer, New York, **2008**, pp. 89 – 189.
[3] C. Delacourt, P. L. Ridgway, J. B. Kerr, J. Newman, *J. Electrochem. Soc.* **2008**, *155*, B42.
[4] A. A. Peterson, J. K. Nørskov, *J. Phys. Chem. Lett.* **2012**, *3*, 251 – 258.
[5] D. T. Whipple, P. J. A. Kenis, *J. Phys. Chem. Lett.* **2010**, *1*, 3451 – 3458.
[6] C. Costentin, M. Robert, J.-M. Savéant, *Chem. Soc. Rev.* **2013**, *42*, 2423 – 2436.
[7] J. Qiao, Y. Liu, F. Hong, J. Zhang, *Chem. Soc. Rev.* **2014**, *43*, 631 – 675.
[8] Y. Hori, A. Murata, R. Takahashi, *J. Chem. Soc. Faraday Trans. 1* **1989**, *85*, 2309 – 2326.
[9] M. Gattrell, N. Gupta, A. Co, *Energy Convers. Manage.* **2007**, *48*, 1255 – 1265.
[10] C. Amatore, J. M. Saveant, *J. Am. Chem. Soc.* **1981**, *103*, 5021 – 5023.
[11] A. A. Peterson, F. Abild-Pedersen, F. Studt, J. Rossmeisl, J. K. Nørskov, *Energy Environ. Sci.* **2010**, *3*, 1311.
[12] M. Gattrell, N. Gupta, A. Co, *J. Electroanal. Chem.* **2006**, *594*, 1 – 19.
[13] R. Kortlever, J. Shen, K. J. P. Schouten, F. Calle-Vallejo, M. T. M. Koper, *J. Phys. Chem. Lett.* **2015**, *6*, 4073 – 4082.
[14] B. Kumar, J. P. Brian, V. Atla, S. Kumari, K. A. Bertram, R. T. White, J. M. Spurgeon, *ACS Catal.* **2016**, *6*, 4739 – 4745.
[15] K. P. Kuhl, E. R. Cave, D. N. Abram, T. F. Jaramillo, *Energy Environ. Sci.* **2012**, *5*, 7050.
[16] Y. Hori, R. Takahashi, Y. Yoshinami, A. Murata, *J. Phys. Chem. B* **1997**, *101*, 7075 – 7081.
[17] R. Shiratsuchi, G. Nogami, *J. Electrochem. Soc.* **1996**, *143*, 582 – 586.
[18] C. F. C. Lim, D. A. Harrington, A. T. Marshall, *Electrochim. Acta* **2017**, *238*, 56 – 63.
[19] N. Gupta, M. Gattrell, B. MacDougall, *J. Appl. Electrochem.* **2006**, *36*, 161 – 172.
[20] Y. Hori, H. Konishi, T. Futamura, A. Murata, O. Koga, H. Sakurai, K. Oguma, *Electrochim. Acta* **2005**, *50*, 5354 – 5369.
[21] E. Protopopoff, P. Marcus, *Electrochim. Acta* **2005**, *51*, 408 – 417.
[22] J. Heyes, M. Dunwell, B. Xu, *J. Phys. Chem. C* **2016**, *120*, 17334 – 17341.
[23] M. Dunwell, Q. Lu, J. M. Heyes, J. Rosen, J. G. Chen, Y. Yan, F. Jiao, B. Xu, *J. Am. Chem. Soc.* **2017**, *139*, 3774 – 3783.
[24] C. M. Gunathunge, X. Li, J. Li, R. P. Hicks, V. J. Ovalle, M. M. Waegele, *J. Phys. Chem. C* **2017**, *121*, 12337 – 12344.
[25] C. W. Li, M. W. Kanan, *J. Am. Chem. Soc.* **2012**, *134*, 7231 – 7234.
[26] K. P. Kuhl, T. Hatsukade, E. R. Cave, D. N. Abram, J. Kibsgaard, T. F. Jaramillo, *J. Am. Chem. Soc.* **2014**, *136*, 14107 – 14113.
[27] J. Yano, S. Yamasaki, *J. Appl. Electrochem.* **2008**, *38*, 1721 – 1726.
[28] A. J. Bard, L. R. Faulkner, *Electrochemical methods: fundamentals and applications, 2nd ed.*, Wiley, New York, **2001**.

Manuscript received: February 11, 2018
Revised manuscript received: April 21, 2018
Version of record online: May 22, 2018